AIDIC *Conference Series*, Vol. 9, 2009
Editor Sauro Pierucci
DOI: 10.3303/ACOS0909011

ISBN 978-88-95608-10-5 ISSN 2036-5969

PLATINUM CATALYSTS FOR THE LOW TEMPERATURE CATALYTIC STEAM REFORMING OF ETHANOL

Paolo Ciambelli[a], Vincenzo. Palma[a*], Arianna Ruggiero[a], Gaetano. Iaquaniello[b]

[a]Dipartimento di Ingegneria Chimica e Alimentare, Università degli Studi di Salerno, Via Ponte Don Melillo, 84084 Fisciano (SA), Italy
[b]Technip KTI S.p.A., Viale Castello della Magliana 75, 00184 Roma, Italy

Electric power generation by H_2 fuel cells is the most promising technology for the reduction of fossil fuels dependence, greenhouse gas emissions and atmospheric pollution. Among different H_2 sources ethanol is very attractive when obtained from biomass minimizing CO_2 emissions. At low temperature ethanol steam reforming to H_2 or pre-reforming to CH_4 can increase the overall system efficiency, but the by-products formation leads to reduced selectivity and catalyst durability because of coke formation. The feasibility of this process is strictly correlated to both technological and economical aspects. In this work the performance of Pt based catalysts supported on Al_2O_3 and CeO_2 has been studied and compared in terms of catalytic activity and selectivity in the temperature range 300-450 °C. Moreover the techno-economic feasibility of green energy production via steam reforming of bio-ethanol (ESR) was evaluated.

1. Introduction

In the last years H_2 attracts significant research interest because it is a clean fuel without co-production of greenhouse gases. Commercially, hydrogen has been produced from catalytic steam reforming of fossil fuels as methane, as reported by Rostrup-Nielsen (1984). Huber et al. (2003), Cortright et al. (2002), Deluga et al. (2004), reported that to reduce the greenhouse gas emissions, H_2 should be derived from renewable fuels such as bioethanol. As a consequence, ESR has been studied, as it provides an alternative fuel source for hydrogen production. In ESR to produce H_2 for PEM fuel cells, high-reforming temperatures also favor CO formation, which poisons the anode. As a result, CO reduction processes are required. The high-reforming temperature coupled with the lower temperature water gas shift step suffers from thermal inefficiencies. Low temperatures ESR allows high system efficiency and lower hardware construction costs. However, at low temperatures, CH_4 and undesirable byproducts(coke precursors) are thermodynamically favored "Garcia and Laborde (1991), Vasudeva et al. (1996), Fishtik at al. (2000), Mas et al. (2006)", reducing H_2 selectivity and catalyst life. Thus, kinetic rather than thermodynamic control of the reaction is required. Moreover high ethanol conversion is vital for the process economy. On the other hand, since at low temperature CH_4 is thermodynamically favoured, a process strategy is the integration of H_2 production by steam reforming with CH_4 production by pre-reforming; CH_4 could be converted to H_2 in a following steam reforming stage. The feasibility of this process is strictly correlated to both technological and economical aspects. The development of an high performance catalyst able to assure the production of H_2 and CH_4 rich stream by low temperature steam reforming of bio-ethanol, as well as the costs comparison of bio-ethanol steam reforming (ESR) with the conventional steam methane reforming (SMR) process are essential requirements to asses the suitability of the former for clean and renewable energy production. The objective of the present study therefore was to develop a new, highly efficient and cost effective process for green energy production by ethanol steam reforming at low temperature. Therefore the performance in ESR of Pt based catalysts has been studied by varying support (Al_2O_3 and CeO_2), metal loading and

Please cite this article as: Ciambelli P., Palma V., Ruggiero A. and Iaquaniello G., (2009), Platinum catalysts for the low temperature catalytic steam reforming of ethanol, AIDIC Conference Series, 09, 83-92 DOI: 10.3303/ACOS0909011

temperature (300-450 °C). Moreover, the techno-economic feasibility of ESR for energy production was evaluated.

2. Experimental

2.1 Catalyst preparation

Commercially available CeO_2 (Aldrich) and Al_2O_3 (Fisons) with a BET surface area of 80 and 160 m^2/g, respectively, were used as support. Pt-containing catalysts were prepared by impregnating the support with aqueous solution of $PtCl_4$, drying at 120 °C overnight and calcining for 3h in air at 600 °C (dT/dt=10°C/min).

2.2 Catalytic activity testing

Ethanol steam reforming laboratory plant was sketched in Figure 1

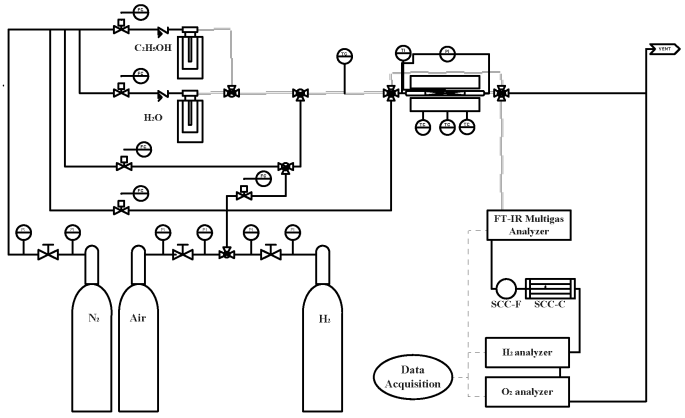

Figure 1. Ethanol steam reforming laboratory plant.

Catalytic activity tests were performed on powder catalyst (180 ÷ 355 μm) in the range 300 ÷ 450°C in a continuous flow fixed bed reactor (18 mm i.d) placed in a three zone electric oven, at atmospheric pressure. Ethanol and water were fed by saturating an N_2 flow at fixed temperature. The mixture was diluted with a N_2 stream, giving a typical feed gas composition of $C_2H_5OH/H_2O/N_2$ = 0.5/1.5/98 vol %. The GHSV was 15000 h^{-1} and the reactor outlet concentrations of C_2H_5OH, H_2O, CH_4, CO, CO_2 and other by-products were monitored with an on line Nicolet Antaris IGS FT-IR multigas analyzer, equipped with an heated gas cell operating at temperatures up to 185 °C and an MCT-A N_2 liquid cooled detector. The dedicated analysis software is able to follow up to 100 different gaseous species simultaneously. The data were acquired at 0.5 cm^{-1}, and cell temperature and pressure were monitored and used to correct gas concentrations. The H_2 and O_2 concentrations in the gas stream were measured respectively by CALDOS 27 and MAGNOS 206, ABB analyzers.

3. Results

3.1 Effect of support and metal loading

The role of the support and metal loading in ethanol steam reforming reaction was examined using Pt as the active metal whose loading was varied from 1 to 3 wt %. The supports have no activity in ethanol steam reforming reaction as appeared from the test carried out at 300 °C (not reported). Ethanol conversion and hydrogen yield as function of time on stream for Pt based catalysts tested are reported in Figure 2. For Pt/CeO_2 catalysts a transient time is observed in the ethanol conversion behaviour. Experimental results show that the time required to reach the apparent ethanol complete conversion decreases by increasing Pt loading, it disappears for the highest metal content.

For the 1-Pt/Al_2O_3 sample it is observed a similar tendency of 1-Pt/CeO_2 catalytic system, even if a lower H_2

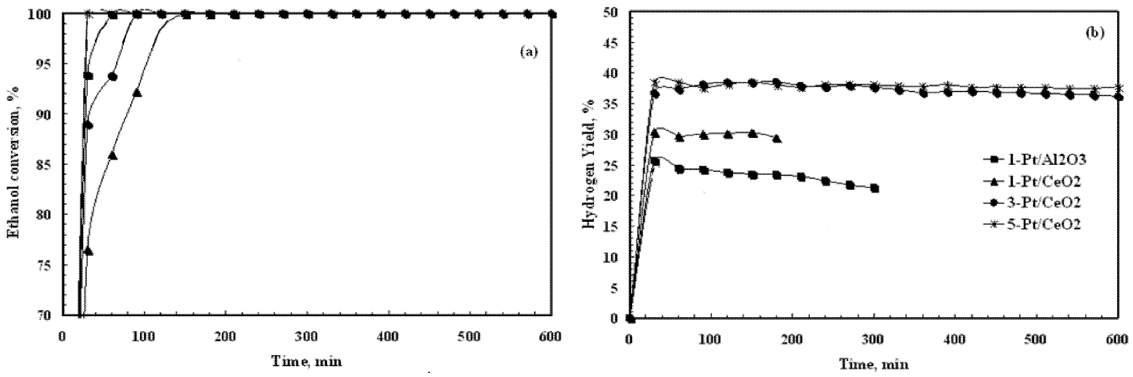

Figure 2. Ethanol conversion (a) and hydrogen yield (b) in ESR on CeO_2 and Al_2O_3 supported Pt catalysts with different metal loading versus time on stream. Experimental conditions: T = 300 °C, EtOH = 0.5 vol%, EtOH:H_2O:N_2 = 0.5:1.5:98, Total gas flow rate= 1000 (stp)cm^3/min, GHSV = 15000 h^{-1}.

yield is observed. Hydrogen yield is higher and more stable for Pt/CeO_2 catalysts in respect to Pt/Al_2O_3 catalysts, moreover on both supports it increases with metal loading. In contrast with the conversion behavior, in the H_2 yield curves, no transient time is observed. Products distribution was strongly influenced from the nature of the support and the metal loading. In Table 1 is shown the selectivity of reaction products. H_2 and CO_2 selectivity are higher on Pt/CeO_2 catalysts; the samples with the higher metal content are the most selective to CO_2 and H_2 among the systems examined. CO selectivity is lower on Pt/CeO_2 catalysts; no formation of CO is detected on 5-Pt/CeO_2. Pt/Al_2O_3 catalyst is more selective to CH_4 and CO; CH_4 selectivity increases on Pt/CeO_2 by increasing metal content. The selectivity to H_2, CO and CO_2 are related via the water gas shift reaction, while the selectivity toward CH_4 is independent of that and is related only to the ethanol decomposition and steam reforming reactions. Based on product distribution results, the catalytic systems examined have not the same WGS activity, Pt/CeO_2 is much more active than Pt/Al_2O_3 catalyst. The activity in WGS reaction is enhanced by increasing metal loading.

Table 1. Products distribution in ESR on CeO_2 and Al_2O_3 supported Pt catalysts with different metal loading. Experimental conditions: T = 300 °C, EtOH = 0.5 vol%, EtOH:H_2O:N_2 = 0.5:1.5:98, Total gas flow rate= 1000 (stp)cm^3/min, GHSV = 15000 h-1, Time on stream = 3 h.

Catalyst	S_{CH4} (%)	S_{CO}(%)	S_{CO2}(%)	S_{H2} (%)	S_{C2H4} (%)	S_{C3H6O} (%)	S_C (%)
1-Pt/Al_2O_3	39.3	45.2	4.0	23.4	9	-	-
1-Pt/CeO_2	31.5	21.0	25.8	29.5	-	16.2	-
3-Pt/CeO_2	43.5	1.6	56.4	38.6	-	1.2	-
5-Pt/CeO_2	40.2	0	58.8	38.0	-	-	-
Equilibrium	56	0	33	18	0	0	10

Selectivity were calculated according to the following equations:

$$S_i = \frac{n_i/2}{n^{in}_{C2H5OH} - n^{out}_{C2H5OH}} \quad \text{where } i \text{ is } CO, CO_2 \text{ and } C;\quad S_{H2} = \frac{n_{H2}/6}{n^{in}_{C2H5OH} - n^{out}_{C2H5OH}};\quad S_{CH3CHO} = \frac{n_{CH3CHO}}{n^{in}_{C2H5OH} - n^{out}_{C2H5OH}};\quad S_{C2H4} = \frac{n_{C2H4}}{n^{in}_{C2H5OH} - n^{out}_{C2H5OH}};$$

The main secondary products observed on the catalysts tested are ethylene on Pt/Al_2O_3 and acetone on Pt/CeO_2.

3.2 Effect of temperature

The effect of temperature was also investigated. The results, in terms of conversion, yield and selectivity as function of temperature, of 5-Pt/CeO_2 catalyst, are shown in Table 2.

Ethanol conversion was always complete, while water conversion and H_2 yield increase from 300 to 450 °C.

The overall H_2 production increases with temperature, but at higher temperature CH_4 selectivity decreases, and trace amounts of CO compare, likely due to the occurrence of CH_4 steam reforming reaction. For this reason, intermediate temperatures allows high H_2 and CH_4 production, and minimize CO formation.

Table 2. Effect of temperature on ethanol and water conversion, H_2 yield and products distribution in ESR on 5-Pt/CeO_2 catalyst. T = 300 °C, EtOH = 0.5 vol%, EtOH:H_2O:N_2 = 0.5:1.5:98; Gas flow rate = (stp)1000 cm^3/min, GHSV = 15000 h^{-1}, Time on stream = 3 h.

Temperature, °C	X_{EtOH} (%)	X_{H2O}(%)	Y_{H2}(%)	S_{CH4} (%)	S_{CO}(%)	S_{CO2}(%)	S_{H2} (%)
300	100	30.2	38	40.2	0	58.8	38.0
350	100	43.4	44.3	38.8	0	60.2	44.3
450	100	52.4	65.1	29.1	4.0	61.8	65.1

3.3 Physical and chemical characterization

The values of specific surface area of both supports and catalysts with their nominal metal content are listed in Table 3. The BET surface area of calcined CeO_2 was 46 m^2/g. Upon platinum loading the specific surface area decreased to 35 m^2/g for 3-Pt/CeO_2, while it increased to 54 m^2/g for Pt 5 wt % loading. In the case of alumina SSA was unchanged at lower platinum loading, while it increased to 187 m^2/g for 1- Pt/Al_2O_3.

Table 3. Nominal metal content and specific surface area (SSA) of Al_2O_3 and CeO_2 supported catalysts.

Samples	Nominal metal content, wt %	SSA, m^2/g
Al_2O_3	-	160
CeO_2	-	46
1- Pt/Al_2O_3	1	187
1-Pt/CeO_2	1	47
3-Pt/CeO_2	3	35
5-Pt/CeO_2	5	54

XRD diffraction patterns of Al_2O_3 and 1 % Pt/Al_2O_3 samples after calcination are shown in Figure 3. For 1-Pt/Al_2O_3, only peaks assigned to γ-Al_2O_3 are observed, suggesting that Pt is well dispersed on the support surface. XRD diffraction patterns of Pt/CeO_2 samples after hydrogen reduction are shown in Figure 4 (a) and (b). All spectra did not show the characteristic signals from metallic platinum at $2\theta = 39.9$ and 47.0, likely due to high metal dispersion on the support. Only CeO_2 signals corresponding to a fluorite-like structure ($2\theta = 28.5, 33.3, 47.5, 56.4$) were present. However, a deeper analysis of XRD spectra in the range 27-30 2θ shows reflections less intensive and slightly shifted to higher 2θ values with respect to pure CeO_2. Moreover, the extent of shifting and the reduction of intensity increase with increasing the platinum loading.

The apparent crystallite size (*d*) was evaluated by the Scherrer equation: $d = \frac{k\lambda}{\beta \cos\theta}$

The lattice parameter *a* of the samples was calculated from the equation: $a = \sqrt{h^2 + k^2 + l^2}\left(\frac{\lambda}{2sen\theta}\right)$

The unit cell volume was calculated considering the CeO_2 cubic structure: $V = a^3$

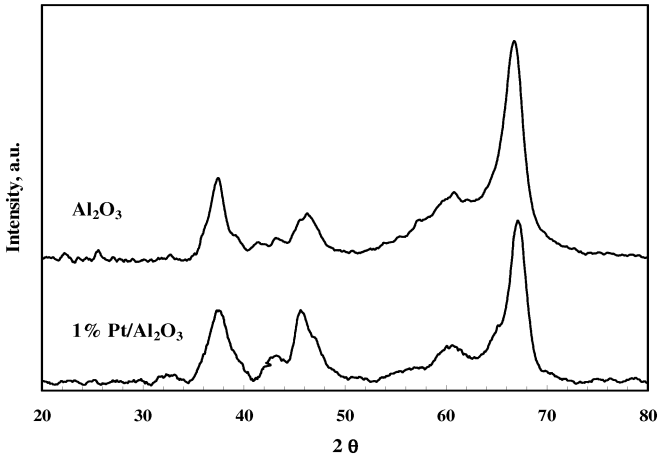

Figure 3. XRD patterns of Al_2O_3 and 1% Pt/Al_2O_3 after calcination.

Four main peaks corresponding to the (1 1 1), (2 0 0), (2 2 0) and (3 1 1) CeO_2 reflecting planes were taken into account for the calculations. The results are reported in Table 4.

Table 4. Physical properties of Pt/CeO_2 catalysts.

Samples	**d, Å**		**a, Å**		**V, Å^3**	
	calcined	Reduced	calcined	reduced	calcined	reduced
CeO_2	217	219	5.411	5.405	158.4	157.9
3% Pt/CeO_2	258	230	5.404	5.396	157.8	157.1
5% Pt/CeO_2	279	274	5.382	5.387	155.9	156.3

The ceria crystallite size is something increased upon Pt loading, while a contraction of cell volume at increased metal loading is observed. Similar values were obtained with reduced catalysts. The formation of a solid solution by replacement of Ce^{4+} with Pt^{4+} or Pt^{2+} in the ceria lattice may determine a lattice shrinkage which accounts for the smaller cation radius of Pt^{4+} or Pt^{2+} (ionic radius = 0.625 or 0.80 Å) with respect to Ce^{4+} (ionic radius = 0.97 Å). Probably the partial incorporation of Pt in the CeO_2 structure, causing the observed lattice shrinkage, results in a $-O^{2-}-Ce^{4+}-O2^{-}-Pt^{2+/4+}-O^{2-}$ linkages on the ceria surface with the creation of oxygen ion vacancies.

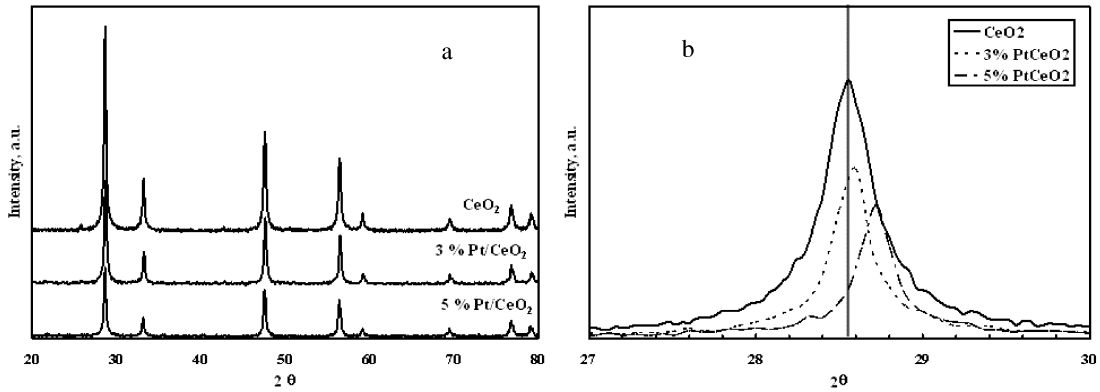

Figure 4. (a) XRD patterns of Pt/CeO_2 catalysts after reduction treatment, (b) particular of XRD patterns of Pt/CeO_2 catalysts.

Temperature programmed reduction test.
The sample 1-Pt/Al_2O_3 shows a first peak at 105 °C, a broad composite peak centered at 245 °C and a small peak centered at 393 °C. The relative contributions to the hydrogen uptake, as calculated after peaks deconvolution (Figure 5), are reported in Table 5.

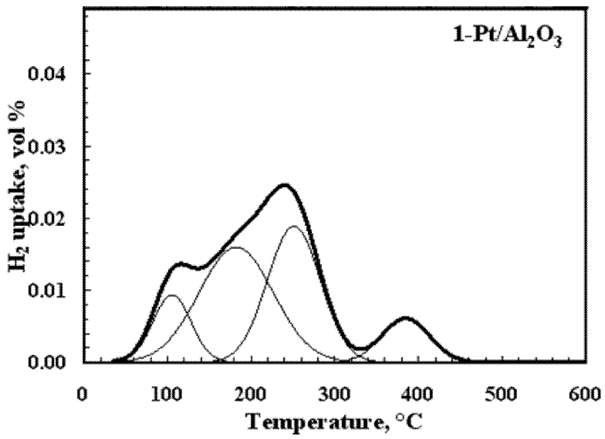

Figure 5. TPR profiles of Pt/Al_2O_3 catalysts.

In agreement with C. Hwang *et al.* (1996), we assigned the lower temperature peaks to the reduction of PtO_2 species. Since the hydrogen uptake for 1 wt % metal loading is lower than that required for the reduction of PtO_2, we may explain this behavior considering that platinum could be simultaneously present as metallic, as PtO, and also as Pt oxychlorinated species, that are reduced at higher temperature, as reported by H. Lieske *et al.* (1983).

Table 5. TPR H_2 uptake of Pt/ Al_2O_3 catalyst.

	T, °C	*H_2, μmol/g*	*H_2, μmol/g for $Pt^{+4} \rightarrow Pt^0$*
1-Pt/Al_2O_3	105	3.8	102
	182	9.2	
	251	6.4	
	384	2.0	

Results of TPR of Pt/CeO_2 catalysts are reported in Figure 6. In the lower temperature range (T<300°C) the profile of 1-Pt/CeO_2 exhibits a single symmetric reduction peak centered at 203 °C, indicating the high dispersion of Pt particles with uniform particle size distribution. By increasing the metal loading to 3 and 5 wt %, the peak area increases and the peak temperature shifts to lower value, while on 5-Pt/CeO_2 a new peak, centered at 90 °C, clearly appears. A similar peak is present as a shoulder in the TPR profile of 3-Pt/CeO_2. In the higher temperature range (T>300°C) two peaks at 366 and 462 °C are observed for 1-Pt/CeO_2. By increasing the platinum content the intensity of the first peak decreases while that of the second increases. At the highest Pt loading (5 wt %) the two peaks are merged in a single one centered at 448 °C. Since pure CeO_2 shows a peak at 480 °C, characteristic of the reduction of capping oxygen anions attached to a surface Ce^{4+} ion, in agreement with H. C. Yao et al. (1984), and C. de Leitenburg et al. (1997), we conclude that the presence of platinum modifies the features of the ceria reduction and suggest the presence of an H_2 spillover mechanism from Pt surface to CeO_2 surface, enhanced by the high metal dispersion on the support surface. The partial amounts of hydrogen uptake, calculated by integrating the peak areas after deconvolution, are reported in Table 6.

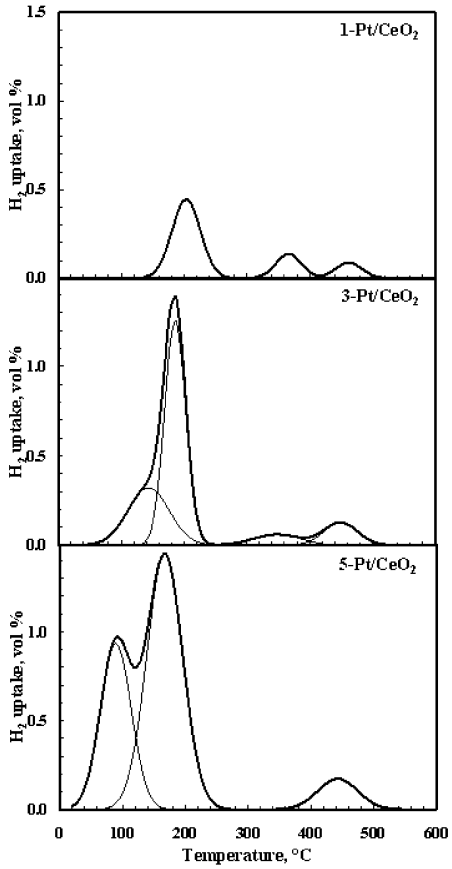

Figure 6. TPR profiles of Pt/CeO_2 catalysts.

Table 6. TPR H_2 uptake of Pt/CeO_2 catalysts.

	T, °C	*H_2, μmol/g*	*H_2, μmol/g for $Pt^{+4} \rightarrow Pt^0$*
1-PtCeO₂	203	117.4	103
	366	32.8	-
	462	22.8	-
3-PtCeO₂	139	137.3	-
	190	286.5	309
	349	28.7	-
	449	41.8	-
5-PtCeO₂	90	212.8	
	180	323.6	515
	448	42.1	-

From this data (Figure 6 and Table 6) it is observed that the amount of hydrogen consumed in the temperature range from RT to 300°C, are in good agreement with the nominal H_2 required for the stoichiometric reduction $Pt^{+4} \rightarrow Pt^0$ reaction.

For what concerns the complexity of the TPR behaviour, we can say that in the literature has been shown by R.W. McCabe et al.(1988), that the reduction temperature of platinum oxides depends primarily of the degree of crystallinity of the oxide (the lower the temperature, the more crystalline the oxide), of the particle size, and of the interaction with the support. In particular, R.R. Rajaram *et al.* (1999) proposed that the formation of a Pt-Ce

solid solution induces the generation of oxygen vacancies, which adsorb oxygen easily. These very reactive oxygen species can be easily reduced by H_2 at low temperatures. From these considerations we can assume that XRD-undetectable particles and strong metal–support interaction or solid solution formation of platinum with ceria lattice (as suggested from XRD analysis) could be responsible for the observed reduction profile and the increase of the specific surface area in the 5 Pt-CeO_2 sample.

4. Techno-economic evaluation

Figure 7 depicts a preliminary block diagram where the heat to convert the ethanol at low temperature is extracted from the sensible heat of the flue gases generated by reforming the methane left over. By such integration export steam can be minimised and the conventional reforming section becomes only a fraction of what required for an equivalent hydrogen production based on natural gas. In Table 7 some technical and economic features are compared together with the Capital Investment (ISBL) for the hybrid ESR+SR and conventional SR.

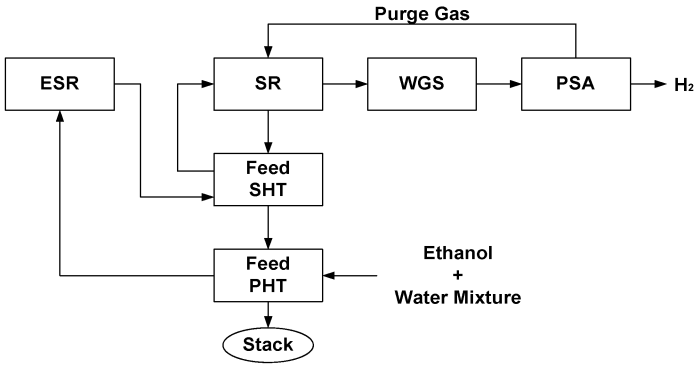

Figure 7. Block diagram of ESR-SR hybrid system

For the same hydrogen capacity the hybrid scheme should cost only 80 % of conventional SR, due to the reduction of the reforming section and elimination of desulphurisation section.

Table 7. Technical and economic data for SR and SR + ESR technology

Technology	SR	ESR + SR
Capacity, Nm^3/h H_2	1500	1500
Reforming section duty, Mkcal/h	1417	1205
Feed	620 Nm^3/h of Natural gas	784 kg/h of Ethanol
Capital investment, million of €	5,0	4,0 (1)

(1) based on reforming section with 85 % of a conventional one and elimination of the desulfurization section

In Table 8 a tentative production cost is calculated using for the variable cost only the cost of feed and for the fixed cost it has been assumed a working life of 15 years and a return on investment (WACC) of 9,5%.

Table 8. Production costs

Technology	SR	SR + ESR
Variable costs	0.062 (1)	0.073
Fixed costs	0.051 (2)	0.040
Éroduction costs, € perNm^3 H_2	0.113	0.113

(1) $\frac{620}{1500} \times 0.15$ € for Nm^3 H_2; (2) Capital Investment / (8400 x 1500 x 7.828); 7.828 = (annuity factor).

From such data the cost of the ethanol mixture which makes the production cost equal to natural gas based, has been calculated. At 0.14. Euro per kg of ethanol in a water ethanol mixture, the production makes an economic

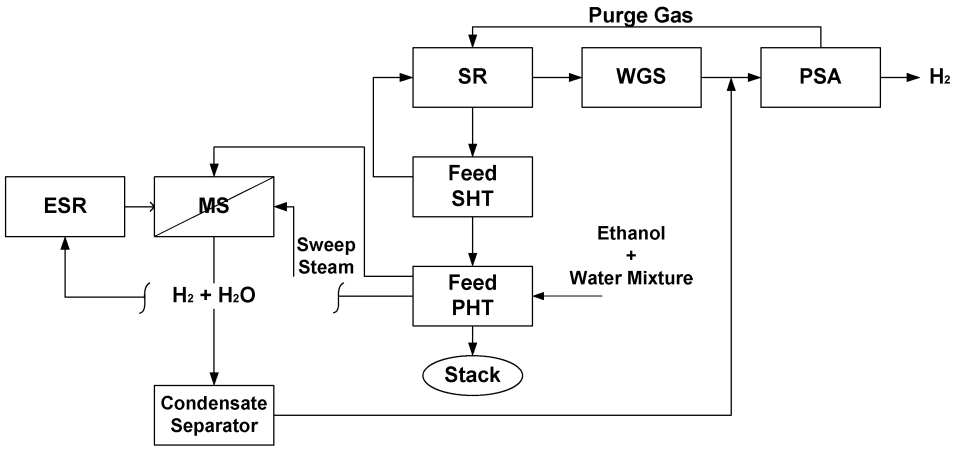

Figure 8. Block diagram of ESR-SR hybrid system with H_2 selective membrane separator

sense and becomes attractive. A more advanced scheme is presented in Figure 4, where between the EPS reactor and the conventional methane reformer, a H_2 selective membrane module is inserted. In such a scheme H_2 produced in the pre-reformer step is recovered before entering the second reforming step, enhancing the CH_4 conversion, reducing the Capital Investment.

5. Conclusions

ESR test performed in the range 300-450 °C on different catalyst showed the relevance of the support and metal loading on the final performances in terms of activity, selectivity and durability. In particular, 5-Pt/CeO_2 sample allow a complete ethanol conversion without C formation in the whole temperature range. The chemical-physical catalysts characterization, together with TPR and TPD tests, showed that the Ceria support stabilize the Pt in a higher oxidation state, with a very high oxide dispersion and strong metal-support interaction, resulting more active and stable with respect to the Al_2O_3 supported sample.

The economic feasibility of green energy production via steam reforming of bio-ethanol (ESR) was evaluated and two hybrid processes scheme were proposed where the H_2 production cost is only 80 % of conventional SR, due to the reduction of the reforming section and elimination of desulphurisation section.

References

Cortright R. D., Davda R.R., Dumesic J.A., 2002, Hydrogen from catalytic reforming of biomass-derived hydrocarbons in liquid water, Nature 418, 964-967.

Deluga G.A., Salge J.R., Schmidt L.D., Verykios X.E., 2004, Renewable hydrogen from ethanol by autothermal reforming, Science 303, 993-997.

Fishtik I., Alexander A., Datta R., Geana D., 2000, A thermodynamic analysis of hydrogen production by steam reforming of ethanol via response reaction, Int. J. Hydrogen Energy 25, 31-45.

Garcia E. Y., Laborde M. A., 1991, Hydrogen production by steam reforming of ethanol: thermodynamic analysis, Int. J. Hydrogen Energy 16 (5), 307-312.

Huber G.W., Shabaker J.W., Dumesic J.A., 2003, Raney Ni-Sn catalyst for H2 production from biomass-derived hydrocarbons, Science 300, 2075-2077.

Mas V., Kipreos R., Amadeo N., Laborde M., 2006, Thermodynamic analysis of ethanol/water system with the stoichiometric method, Int. J. Hydrogen Energy 31, 21-28.

Rostrup-Nielsen J.R., 1984, Catalysis Science and Technology, vol. 5, Eds. Anderson J. R. and Boudart M., Springer, Berlin.

Vasudeva K., Mitra N., Umasankar P., Dhingra S.C., 1996, Steam reforming of ethanol for hydrogen production: thermodynamic analysis, Int. J. Hydrogen Energy 21 (1), 13-18.

Lieske, H., Lietz, G., Spindler, H. and Volter, J., 1983, Reaction of Platinum in Oxygen and Hydrogen Treated Pt/h-Al2O3 Catalysts, J. Catal., 81, 8-14.

C. Hwang, C. Yeh, J. Mol. Catal. A: Chem., 1996, Platinum-oxide species formed by oxidation of platinum crystallites supported on alumina 112 , 295-302

H. C. Yao, Y. F. Yu Yao, J. Catal., 1984, Ceria in automotive exhaust catalysts : I. Oxygen storage 86, 254-265

C. de Leitenburg, A. Trovarelli, J. Kašpar, J. Catal., 1997, A Temperature-Programmed and Transient Kinetic Study of CO_2 Activation and Methanation over CeO_2 Supported Noble Metals 166, 98-107

R.W. McCabe, C. Wong, H.S. Woo, J. Catal., 1988, The passivating oxidation of platinum 114, 354-367

R.R. Rajaram, J.W. Hayes, G.P. Ansell, H.A. Hatcher, 1999, US Patent 5,993,762